Figures

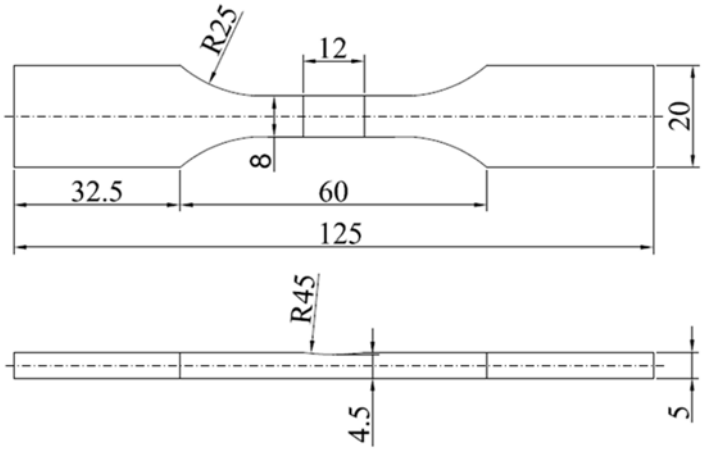

Fig. 1. Schematic of fatigue specimen.

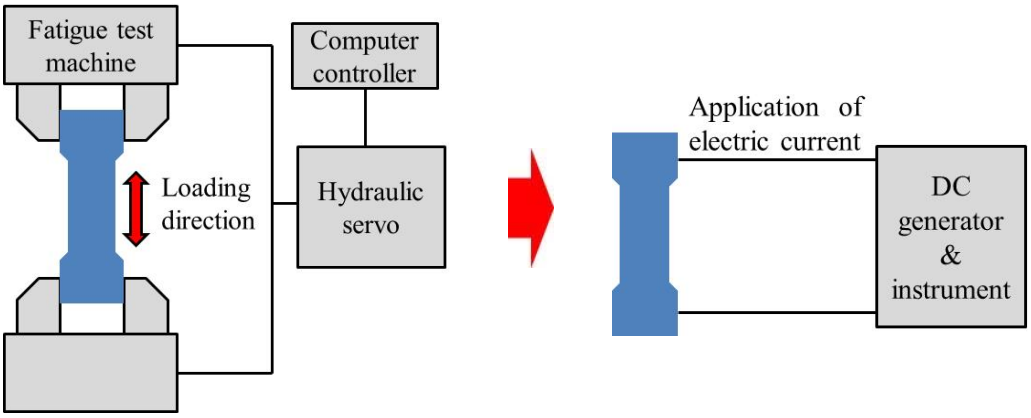

Fig. 2. Schematic of the fatigue test process.

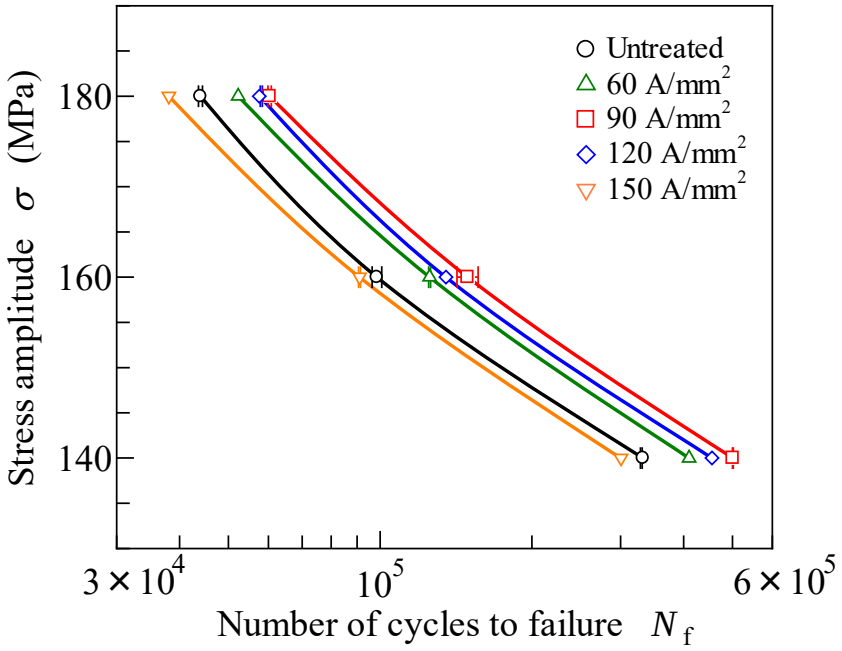

Fig. 3. Relationship between stress amplitude and number of cycles to failure.

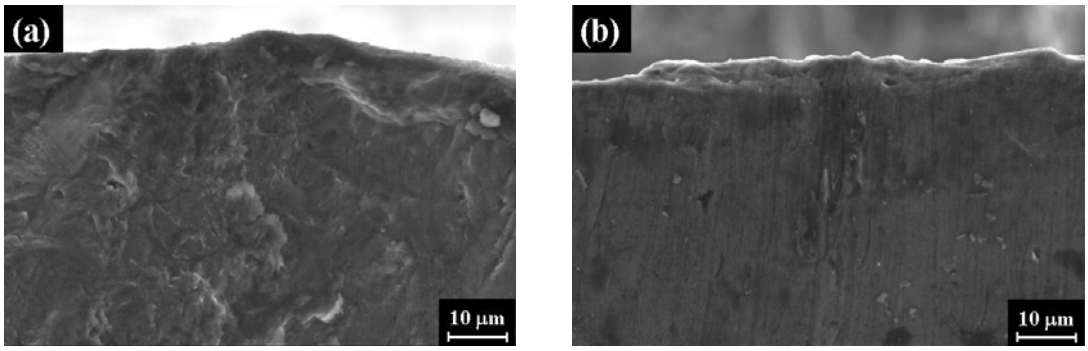

Fig. 4. Scanning electron microscopy (SEM) images of the crack initiation site for the untreated specimen: (a) fracture surface, (b) top surface.

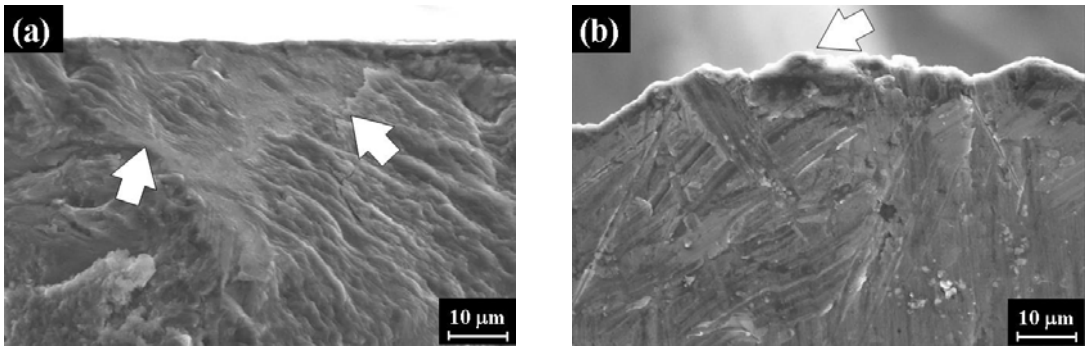

Fig. 5. Scanning electron microscopy (SEM) images of the crack initiation site for the 60-A/mm^2 specimen: (a) fracture surface, (b) top surface. White arrows indicate the local melting sites.

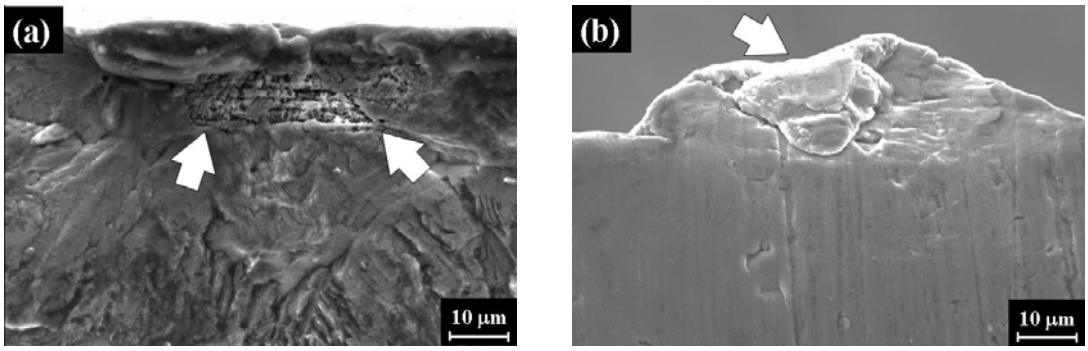

Fig. 6. Scanning electron microscopy (SEM) images of the crack initiation site for the 90-A/mm^2 specimen: (a) fracture surface, (b) top surface. White arrows indicate the local melting sites.

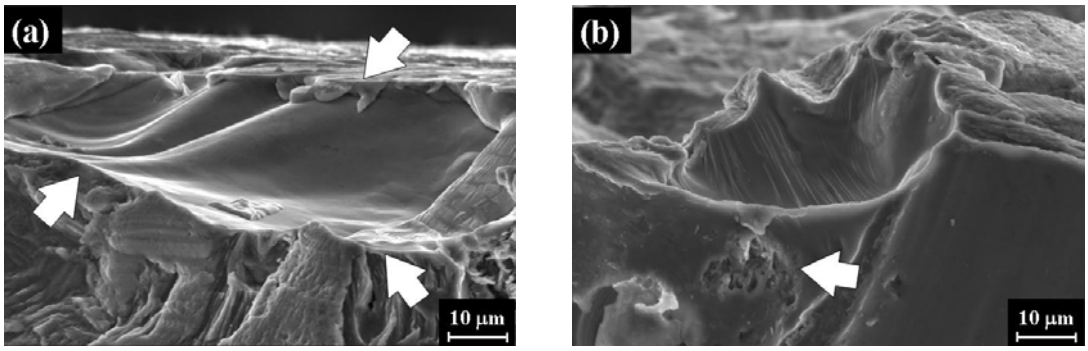

Fig. 7. Scanning electron microscopy (SEM) images of the crack initiation site for the 120-A/mm^2 specimen: (a) fracture surface, (b) top surface. White arrows indicate the local melting sites.

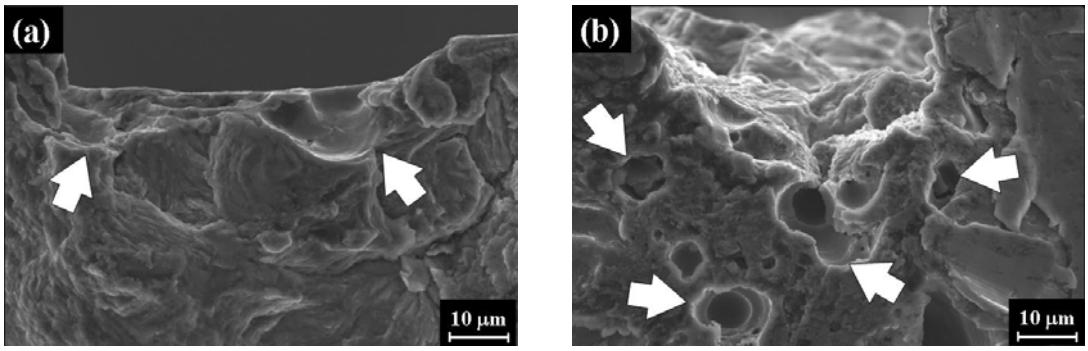

Fig. 8. Scanning electron microscopy (SEM) images of the crack initiation site for the 150-A/mm^2 specimen: (a) fracture surface, (b) top surface. White arrows indicate the local melting sites.

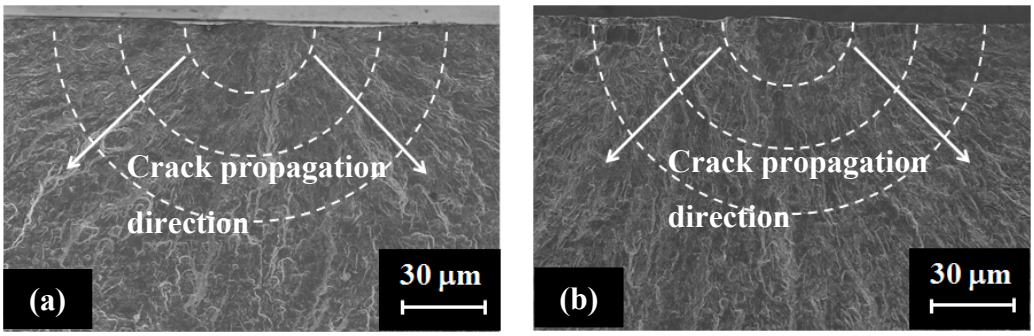

Fig. 9. Scanning electron microscopy (SEM) images of the fracture surface: (a) untreated specimen, (b) 150-A/mm^2 specimen.

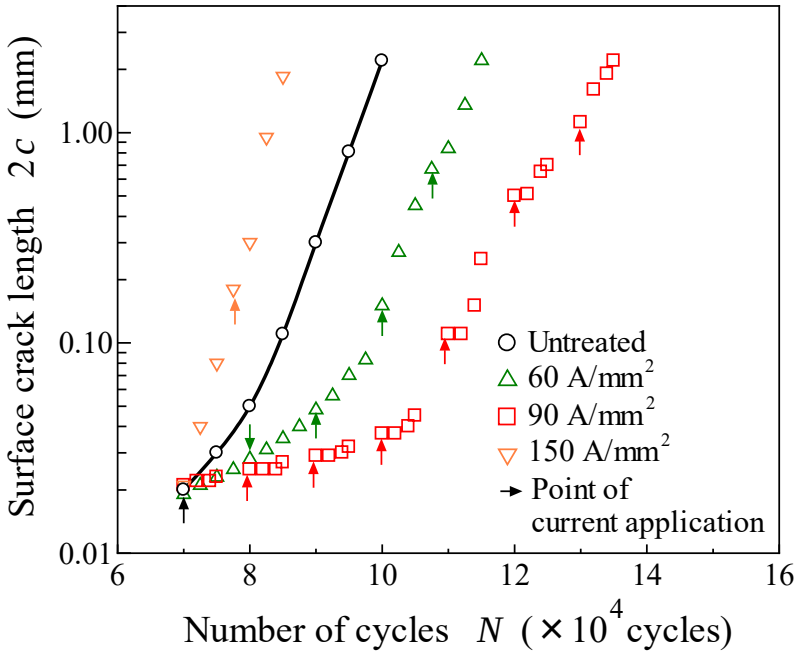

Fig. 10. Relationship between surface crack length and number of cycles.

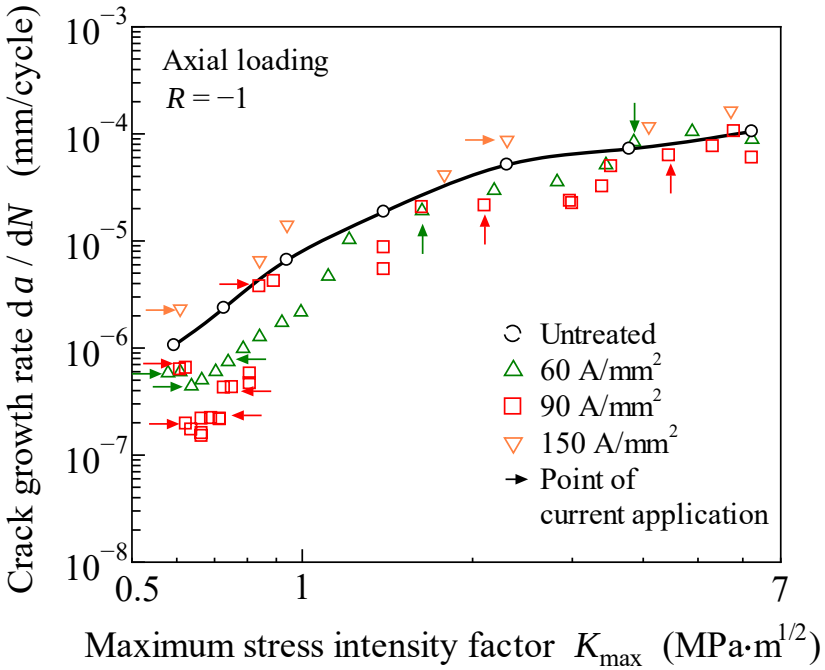

Fig. 11. Crack propagation rate as a function of maximum stress-intensity factor.

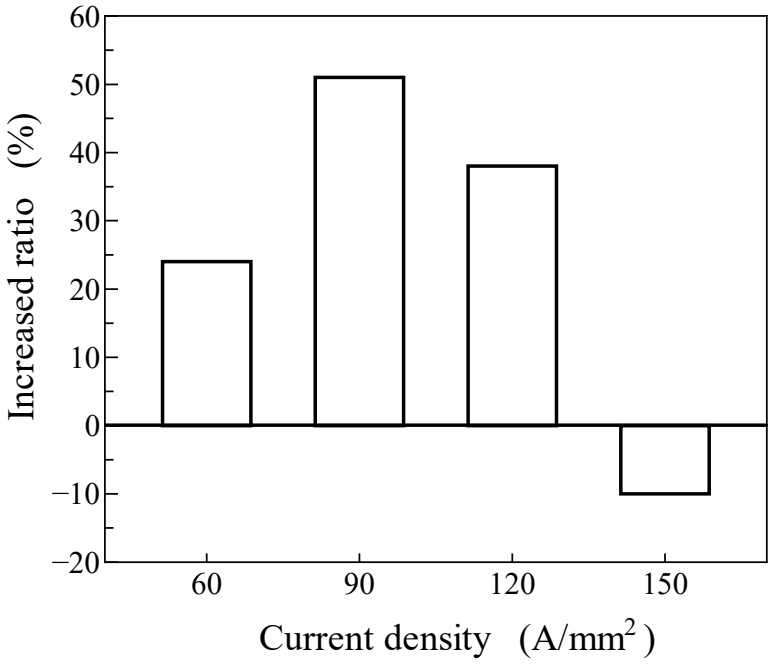

Fig. 12. Increased fatigue life of treated specimens as function of applied electric current (σ = 140 MPa).

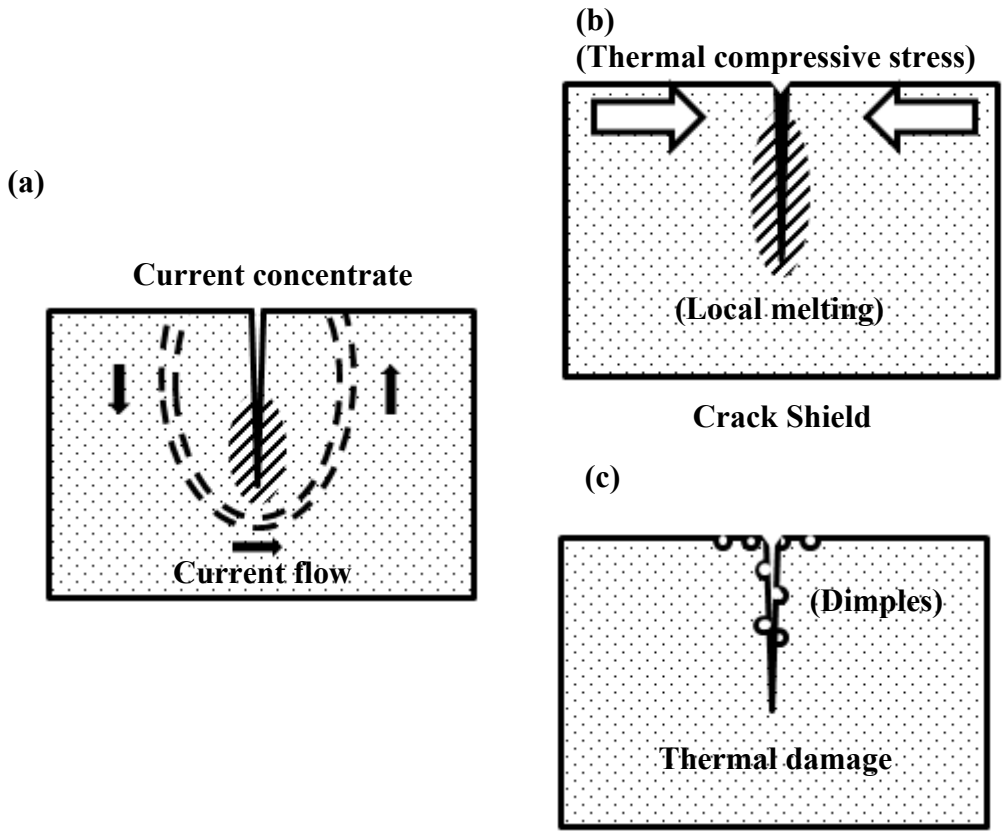

Fig. 13. Schematics depicting the influence of electric current on crack tip at the initiation stage of fatigue cracks: (a) concentration of electric current; (b) crack shield under optimal current densities; (c) thermal damage under overly high current density.